

# LOW-SYMMETRY ASPECTS IN EPR SPECTRA OF $Mn^{2+}$ AT $Bi^{3+}$ SITES IN $BiVO_4$ SINGLE CRYSTAL

T.H. YEOM\*, S.H. CHOH

Department of Physics, Korea University, Seoul 136-701, Republic of Korea

AND CZ. RUDOWICZ†

Department of Applied Science, City Polytechnic of Hong Kong, Hong Kong

(Received June 10, 1992)

Zero-field splitting parameters obtained from EPR X-band experiments of Baran et al. (1985) and Yeom et al. (1992) are reanalyzed. Transformation relations are derived to express the two sets of data in the same axis system. Problems arising from using a truncated zero-field splitting Hamiltonian in fitting the experimental data are elucidated. Low-symmetry aspects in EPR spectra of  $Mn^{2+}$  at  $Bi^{3+}$  sites in  $BiVO_4$  single crystal are considered. Good agreement for orthorhombic parameters  $b_2^0$  and  $b_2^2$  is obtained indicating that the centres observed in the two cases are the same Mn centres. The remaining  $b_k^2$  parameters accounting for the actual site symmetry around  $Mn^{2+}$  impurity which seems to be lower than orthorhombic in the ferroelastic phase cannot be unambiguously determined from the existing EPR data.

PACS numbers: 75.10.Dg, 76.30.Da, 61.16.Hn, 78.20.Hp

## 1. Introduction

Ferroelastics received considerable attention in the recent years. Synthetic bismuth vanadate ( $BiVO_4$ ) may prove to be a promising material for acoustooptics [1, 2].  $BiVO_4$  was first synthesized in 1963 by Roth and Waring [3] and was found to be ferroelastic [4]. Recently, a number of experiments, e.g. X-ray and neutron diffraction [5], Raman scattering [6–8], NMR [9–12], and EPR [13–16] have been carried out to investigate structural changes, phase transitions, and optical properties of  $BiVO_4$ . EPR is a powerful technique in studies of local site symmetry around paramagnetic impurities in crystals. EPR studies of  $Gd^{3+}$ ,  $Er^{3+}$ , and  $Mn^{2+}$  in  $BiVO_4$  single crystals were reported [13–16]. The site symmetry of  $Gd^{3+}$

\*Present address: Department of Applied Science, City Polytechnic of Hong Kong, Hong Kong.

†To whom correspondence should be addressed.

centre in  $\text{BiVO}_4$  single crystal was determined [13]. However, the site symmetry of  $\text{Mn}^{2+}$  centres in  $\text{BiVO}_4$  has not been unambiguously determined as yet.

In the present paper, we reanalyse the zero-field splitting (ZFS) parameters obtained from EPR X-band experiments of Baran's et al. [13] and Yeom's et al. [16]. It appears that the two data sets cannot be directly compared. Transformation relations are derived to express the two data sets in the same axis system. Thus, some problems arising from using a truncated ZFS Hamiltonian in fitting the experimental data [16] can be elucidated. Low-symmetry [17] aspects in EPR spectra of  $\text{Mn}^{2+}$  at  $\text{Bi}^{3+}$  sites in  $\text{BiVO}_4$  single crystal are considered. Good agreement between Baran's et al. [13] and Yeom's et al. [16] data for orthorhombic parameters  $b_2^0$  and  $b_2^2$  is now obtained. This indicates that the centres observed in the two cases are the same Mn centres. The remaining  $b_k^q$  parameters accounting for the actual site symmetry around  $\text{Mn}^{2+}$  impurity which seems to be lower than orthorhombic in the ferroelastic phase cannot be unambiguously determined from the existing EPR data. The present results may lead to a more reliable determination of the site symmetry for other  $\text{Mn}^{2+}$  impurity centres in  $\text{BiVO}_4$  as well as for monoclinic and triclinic EPR centres in other crystals.

## 2. Crystal structure

$\text{BiVO}_4$  undergoes a reversible second-order phase transition at  $T_c \approx 528$  K from the monoclinic fergusonite to tetragonal schellite structure [18]. The structure is reported [19–21] as given by the point group  $2/m$  ( $C_{2h}$ ) in the ferroelastic phase and  $4/m$  ( $C_{4h}$ ) in the paraelastic phase, respectively. However, no indication was provided on the site (Bi or Mn) to which this determination is referred to.

The structural parameters for  $\text{BiVO}_4$  are  $a = c = 5.1507$  Å,  $b = 11.730$  Å, and  $\beta = 90.0^\circ$  in the paraelastic tetragonal phase at 573 K, whereas  $a = 5.1966$  Å,  $b = 11.704$  Å,  $c = 5.0921$  Å, and  $\beta = 90.38^\circ$  in the ferroelastic phase at room temperature [5]. In the ferroelastic phase the vanadium ions with different bond lengths are located in a distorted oxygen tetrahedron, and the bismuth ions are coordinated by eight distorted  $\text{VO}_4$  tetrahedra. The displacements of  $\text{Bi}^{3+}$  and  $\text{V}^{5+}$  are along the  $b$ -axis and both cations move in the same direction [22]. The displacements of the  $\text{Bi}^{3+}$  ions play a major role in the ferro- to paraelastic phase transition [23].

## 3. Spin Hamiltonian for low-symmetry EPR centres

EPR determination [15] indicates that  $\text{Gd}^{3+}$  and  $\text{Mn}^{2+}$  ions enter  $\text{Bi}^{3+}$  site and the site symmetry for  $\text{Gd}^{3+}$  centres is given by point group  $S_4$  at  $T > T_c$  and  $C_2$  at  $T < T_c$ . Two types of  $\text{Mn}^{2+}$  centres, namely  $\text{Mn}_I$  — remotely compensated and  $\text{Mn}_{II}$  — locally compensated centres, were detected at  $T < T_c$  and interpreted using a monoclinic spin Hamiltonian [15]. The zero-field splitting Hamiltonian [24] in terms of the extended Stevens [25, 26] operators for spin  $S = 5/2$  has the following form for these cases:

— tetragonal symmetry type II (groups:  $C_4$ ,  $S_4$ ,  $C_{4h}$ ):

$$\mathcal{H}_{\text{ZFS}} = B_2^0 O_2^0 + B_4^0 O_4^0 + B_4^4 O_4^4 + B_4^{-4} O_4^{-4}, \quad (1)$$

— orthorhombic symmetry (groups:  $D_2$ ,  $C_{2v}$ ,  $D_{2h}$ ):

$$\mathcal{H}_{ZFS} = B_2^0 O_2^0 + B_2^2 O_2^2 + B_4^0 O_4^0 + B_4^2 O_4^2 + B_4^4 O_4^4, \quad (2)$$

— monoclinic symmetry (groups:  $C_2$ ,  $C_{1h}(C_s)$ ,  $C_{2h}$ ) — assuming the monoclinic  $C_2$  axis is parallel to the  $z$ -axis:

$$\mathcal{H}_{ZFS} = \mathcal{H}_{ZFS}(\text{ortho}) + B_2^{-2} O_2^{-2} + B_4^{-2} O_4^{-2} + B_4^{-4} O_4^{-4}. \quad (3)$$

Two other equivalent forms of monoclinic ZFS Hamiltonian should be considered if the magnetic axis  $x$  or  $y$  is chosen as parallel to the monoclinic  $C_2$  axis [27, 28]. Standardization of orthorhombic [29, 30] and monoclinic ZFS (as well as crystal field) Hamiltonian [27] should be considered if the experimental value of the ratio  $B_2^2/B_2^0$  is outside the “standard” range (0, 1). The “scaling” factors [26] defined by  $B_k^q = f_k b_k^q$ ,  $f_k = 1/3$ ,  $1/60$ , and  $1/1260$  for  $k = 2, 4$ , and  $6$ , respectively, were used in Refs. [13–15].

## 4. Analysis and discussion

### 4.1. Ferroelastic phase of $BiVO_4$

The ZFS parameters of  $Mn^{2+}$  ions in  $BiVO_4$  [16] were obtained from least squares fitting of the experimental EPR data at room temperature using only three conventional ZFS parameters, namely  $D = 3B_2^0$ ,  $E = B_2^2$ , and  $F = 180B_4^0$ . The truncated ZFS Hamiltonian used in Ref. [16] provided a satisfactory description of the experimental rotation patterns and an evidence that  $Mn^{2+}$  enters Bi sites. However, it does not allow for a detailed investigation of the site symmetry of  $Mn^{2+}$  centres. The values of the corresponding ZFS parameters  $b_k^q$  [16] are different from those of  $Mn_I$  centre reported by Baran et al. [13]. The designation of the principal axes in Ref. [13] was considered in Ref. [16] as improper because it yielded  $b_2^{-2}$  as the largest second-order ZFS parameter. This problem can be resolved considering the standardization of the monoclinic ZFS Hamiltonian [27] as shown below.

On the other hand, the full monoclinic ZFS Hamiltonian (3) was used in [13], however, without specifying the orientation of the monoclinic  $C_2$  axis with respect to the magnetic axes ( $x$ ,  $y$ ,  $z$ ). The parameters  $b_4^{-2}$  and  $b_4^{-4}$  which indicate low symmetry are almost zero within the limits of the experimental error, whereas  $b_2^{-2}$  ( $c_2^2$  in the notation of Ref. [13]) is much larger than  $b_2^0$  and  $b_2^2$  for the  $Mn_I$  centre. This means that in Ref. [13] a “nonstandard” principal axis system was chosen [27, 29] (see below).

The axis systems used in Refs. [13] and [16] are defined in Fig. 1. Note that the designation of the crystallographic system of coordinates ( $a'$ ,  $b'$ ,  $c'$ ) in Ref. [13] corresponds to ( $c$ ,  $a$ ,  $b$ ) adopted in Ref. [16] after Refs. [3, 4, 21]. Thus, the following transformations must be performed in order to obtain the proper conversion of the ZFS parameters. The equivalent ZFS parameters of Yeom et al. [16] expressed in the axis system of Baran et al. [13] are obtained by the transformation  $S_4$  [27, 29] followed by the rotation by  $+45^\circ$  around the  $z$ -axis. The opposite conversion is achieved by the rotation by  $-45^\circ$  around the  $z$ -axis followed by the transformation  $S_5$  [27, 29]. The  $S_4$  and  $S_5$  transformation relations for the orthorhombic and monoclinic ZFS terms can be found in Refs. [29] and

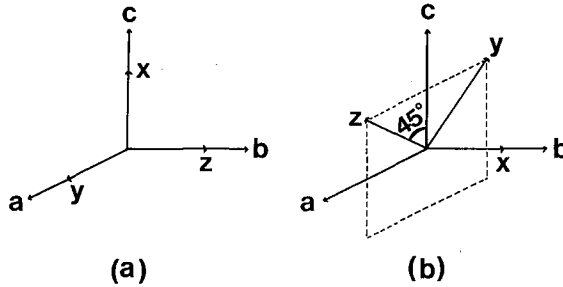


Fig. 1. Definition of the axis system used by (a) Baran et al. [13] and (b) Yeom et al. [16]; (a, b, c) denote the crystallographic axes as defined in [16].

[27], respectively, whereas the relations for the  $\pm 45^\circ$  rotation around the z-axis follow from the general relation, i.e. Eq. (11) in Ref. [31]. The resulting relations in the explicit form may be useful for other low-symmetry cases and are given in Appendix. Using these relations the values in Tables I and II are obtained. It is

TABLE I

The ZFS parameters (in  $10^{-4} \text{ cm}^{-1}$ ) for  $\text{Mn}^{2+}$  in ferroelastic  $\text{BiVO}_4$ : (a) the equivalent of ZFS  $b_k^q$  of Yeom et al. [16] after transformation into the axis system defined by Baran et al. [13]; (b) the original data [13] for comparison.

	$b_2^0$	$b_2^2$	$b_2^{-2}$	$b_4^0$	$b_4^2$	$b_4^4$	$b_4^{-2}$	$b_4^{-4}$
(a)	-161.7 $\pm 0.97$	-	1468.1 $\pm 1.1$	3.9 $\pm 0.1$	-	-45.7 $\pm 0.9$	-26.1 $\pm 0.5$	-
(b)	164 $\pm 2$	-13 $\pm 5$	1460 $\pm 5$	2 $\pm 3$	60 $\pm 15$	1 $\pm 10$	-8 $\pm 10$	2 $\pm 15$

important to consider the “two-way” conversion in the analysis of data [13, 16], since the number of “input” parameters is different in the two cases. Therefore, each conversion leads to a different set of parameters, as it can be seen in Tables I and II. The errors for the transformed  $[b_k^q]$  parameters in Tables I and II were calculated using the formula [30] following from the standard error analysis:

$$[\Delta b_k^q] = \left( \sum_i k_i^2 \{ \Delta b_k^q \}_i^2 \right)^{1/2}, \quad (4)$$

where  $k_i$  are the coefficients in the linear combinations  $[b_k^q] = \sum_i k_i \{ b_k^q \}$  given in Appendix. No transformations are considered for the  $g$ -factor, since in both cases [13, 16] only isotropic  $g$ -value was determined.

The conversion of Yeom's et al. data [16] into the Baran's et al. [13] axis system (Table I) yields instead of the original “standardized” values ( $\{b_2^0\} = 814.9$ ,

TABLE II

The ZFS parameters (in  $10^{-4} \text{ cm}^{-1}$ ) for  $Mn^{2+}$  in ferroelastic  $BiVO_4$ : (a) the equivalent of ZFS  $b_k^q$  of Baran et al. [13] after transformation into the axis system defined by Yeom et al. [16]; (b) the values (a) after the standardization transformation  $S_2$  [27, 29]; (c) the original data [16] for comparison.

	$b_2^0$	$b_2^2$	$b_2^{-1}$	$b_4^0$	$b_4^2$	$b_4^4$	$b_4^{-1}$	$b_4^{-3}$
(a)	648 $\pm 3$	976 $\pm 4$	-26 $\pm 10$	1.6 $\pm 2$	-9.5 $\pm 10$	1.6 $\pm 16$	-14 $\pm 8$	212 $\pm 55$
(b)	-812 $\pm 3$	-484 $\pm 5$	26 $\pm 10$	-0.39 $\pm 3$	-1.6 $\pm 11$	15.5 $\pm 13$	42.5 $\pm 15$	-183.5 $\pm 44$
(c)	814.9 $\pm 0.7$	491.5 $\pm 0.9$	-	10.5 $\pm 0.2$	-	-	-	-

$\{b_2^2\} = 491.5$ ,  $\{b_4^0\} = 10.5$ , in  $10^{-4} \text{ cm}^{-1}$  — see Table II (c)) the nonstandard set with  $\{b_2^{-2}\}$  as the largest parameter and the values of both  $\{b_2^0\}$  and  $\{b_2^{-2}\}$  very close to those obtained by Baran et al. [13]. On the other hand, the original parameter  $\{b_2^{-2}\}$  [13] transforms into  $\{b_2^{-1}\}$  in the axis system of Ref. [16]. The transformed data (a) in Table II turn out to be “nonstandard” and thus require the  $S_2$  transformation [27, 29] to bring them to the standard format (b). This results in the change from the axis system  $(x, y, z)$  into  $(x, z, -y)$  [29]. Again the set (b) in Table II indicates very good agreement with the original values (c) with respect to  $b_2^0$  and  $b_2^2$ , apart from signs. However, the signs were not determined in Ref. [16]. The agreement obtained in the two-way conversion procedure indicates that the Mn centres independently observed by Yeom et al. [16] and Baran et al. [13] are the same  $Mn^{2+}$  centres.

The negative  $q$  ZFS parameters in Tables I and II should account for the low-symmetry effects manifested in the non-coincidence of extrema for resonance between different Zeeman levels [17]. However, practically no low-symmetry effects in the spectra of Mn centres were observed [13]. This was attributed [13] to the smallness of the  $b_4^q$  and  $b_4^{-q}(c_4^m)$ . The ZFS data (b) in Table II support this conclusion. Since the parameter  $b_4^{-3}$  appears to be the strongest, it may be expected that the low-symmetry effects will be most pronounced in the  $|\pm 1/2\rangle$  to  $|\mp 5/2\rangle$  and  $|\pm 3/2\rangle$  to  $|\mp 3/2\rangle$  transitions. The errors of most of the fourth-order ZFS parameters (set (b) in Table II) are greater than or comparable with the magnitude of the parameters, which makes the  $b_4^q$  data [13] unreliable. Nevertheless, the overall behaviour of the low-symmetry ZFS parameters in Table I and II strongly suggests that the site symmetry of  $Mn^{2+}$  centres in  $BiVO_4$  is lower than orthorhombic.

#### 4.2. Paraelastic phase of $BiVO_4$

The ZFS parameters of  $Mn^{2+}$  practically vanish above  $T_c$  [16]. The five fine structure lines which consisted of six lines each, recorded at room temperature,

degenerated into only one with the six-line hyperfine structure in the paraelastic phase. This shows that the effects of spin-orbit coupling interaction of  $Mn^{2+}$  in  $BiVO_4$  crystal are so small that the spacing of energy splitting by the Zeeman term is the same above  $T_c$ . Baran et al. [13] obtained only one ZFS parameter, namely  $b_4^0 = 5b_4^4 = (15 \pm 5) \times 10^{-4} \text{ cm}^{-1}$ , expressed in their crystallographic axis system. Therefore, the tetragonal  $S_4$  distortion around  $Mn^{2+}$  sites seems to be negligible in the paraelastic phase of  $BiVO_4$ .

## 5. Conclusions

The considerations of the low-symmetry aspects in EPR spectra of  $Mn^{2+}$  centres in  $BiVO_4$  reveal that comparison of data from different authors requires careful transformations in the case when the form of spin Hamiltonian and/or the axis systems used are not identical. A two-way transformation procedure for low-symmetry cases is proposed. Using this approach an apparent disagreement between the data of Yeom et al. [16] and Baran et al. [13] was clarified. The transformed values of the second-order zero-field splitting parameters show very good agreement. Therefore, the Mn centres observed in Refs. [13] and [16] are the same centres. The role of the standardization of the spin Hamiltonian parameters, i.e. confining the ratio  $b_2^2/b_2^0$  to the "standard" range (0, 1), is specially evident from our consideration.

Further experimental studies of low-symmetry effects in EPR spectra of  $Mn^{2+}$  and  $Gd^{3+}$  ions in  $BiVO_4$  as well as their temperature dependence are now in progress. More accurate determination of the site symmetry for  $Mn^{2+}$  and  $Gd^{3+}$  centres in the ferroelastic and paraelastic phase of  $BiVO_4$  single crystal may thus be achieved.

## Acknowledgements

This work was partially supported by the Korea Science and Engineering Foundation through the Science Research Center of Excellence Program (1991-1994) and by CPHK research grant.

## Appendix

Two-way conversion relations are given here. The curly brackets denote the original ZFS parameters  $\{B_k^q\}$  in a given axis system, whereas the square brackets denote the equivalent ZFS parameters  $[B_k^q]$  in the transformed axis system. All the relations apply also for the  $b_k^q$  parameters consistently scaled [26] (see also Sec. 3).

The parameters  $\{B_k^q\}$  of Yeom et al. [16] transformed into the axis system defined by Baran et al. [13]:

$$[B_2^2] = \frac{1}{2}\{B_2^{-1}\}, \quad [B_2^1] = \frac{\sqrt{2}}{2}(2\{B_2^{-2}\} + \{B_2^1\}), \quad [B_2^0] = \frac{1}{2}(\{B_2^2\} - \{B_2^0\}),$$

$$[B_2^{-1}] = -\frac{\sqrt{2}}{2}(2\{B_2^{-2}\} - \{B_2^1\}), \quad [B_2^{-2}] = \frac{1}{2}(\{B_2^2\} + 3\{B_2^0\}),$$

$$\begin{aligned}
 [B_4^4] &= -\frac{1}{8}(\{B_4^4\} + 7\{B_4^2\} + 35\{B_4^0\}), \\
 [B_4^3] &= \frac{\sqrt{2}}{2} \left[ \frac{1}{2}(7\{B_4^{-2}\} + 2\{B_4^{-4}\}) - \frac{1}{4}(3\{B_4^3\} + 7\{B_4^1\}) \right], \\
 [B_4^2] &= -\frac{1}{4}(\{B_4^{-1}\} - \{B_4^{-3}\}), \\
 [B_4^1] &= \frac{\sqrt{2}}{2} \left[ -\frac{1}{2}(\{B_4^{-2}\} - 2\{B_4^{-4}\}) + \frac{1}{4}(\{B_4^3\} - 3\{B_4^1\}) \right], \\
 [B_4^0] &= \frac{1}{8}(\{B_4^4\} - \{B_4^2\} + 3\{B_4^0\}), \\
 [B_4^{-1}] &= \frac{\sqrt{2}}{2} \left[ \frac{1}{2}(\{B_4^{-2}\} - 2\{B_4^{-4}\}) + \frac{1}{4}(\{B_4^3\} - 3\{B_4^1\}) \right], \\
 [B_4^{-2}] &= \frac{1}{2}(\{B_4^4\} + \{B_4^2\} - 5\{B_4^0\}), \\
 [B_4^{-3}] &= \frac{\sqrt{2}}{2} \left[ \frac{1}{2}(7\{B_4^{-2}\} + 2\{B_4^{-4}\}) + \frac{1}{4}(3\{B_4^3\} + 7\{B_4^1\}) \right], \\
 [B_4^{-4}] &= \frac{1}{8}(7\{B_4^{-1}\} + \{B_4^{-3}\}).
 \end{aligned}$$

The parameters  $\{B_k^i\}$  of Baran et al. [13] transformed into the axis system defined by Yeom et al. [16]:

$$\begin{aligned}
 [B_2^2] &= \frac{1}{2}(\{B_2^{-2}\} + 3\{B_2^0\}), \quad [B_2^0] = \frac{1}{2}(\{B_2^{-2}\} - \{B_2^0\}), \quad [B_2^{-1}] = 2\{B_2^2\}, \\
 [B_2^1] &= \frac{\sqrt{2}}{2}(\{B_2^1\} + \{B_2^{-1}\}), \quad [B_2^{-2}] = \frac{1}{2\sqrt{2}}(\{B_2^1\} - \{B_2^{-1}\}), \\
 [B_4^4] &= \frac{1}{8}(-\{B_4^4\} + 7\{B_4^{-2}\} + 35\{B_4^0\}), \\
 [B_4^3] &= -\frac{\sqrt{2}}{8} [(-7\{B_4^1\} + \{B_4^{-1}\}) - 3(-\{B_4^3\} + \{B_4^{-3}\})], \\
 [B_4^2] &= \frac{1}{2}(-\{B_4^4\} + \{B_4^{-2}\} - 5\{B_4^0\}), \\
 [B_4^1] &= \frac{\sqrt{2}}{8} [-3(\{B_4^1\} + \{B_4^{-1}\}) + (-\{B_4^3\} + \{B_4^{-3}\})], \\
 [B_4^0] &= \frac{1}{8}(-\{B_4^4\} - \{B_4^{-2}\} + 3\{B_4^0\}), \\
 [B_4^{-1}] &= -\frac{1}{4}(\{B_4^2\} - 2\{B_4^{-4}\}), \\
 [B_4^{-2}] &= \frac{\sqrt{2}}{8} [(\{B_4^3\} + \{B_4^{-3}\}) - (\{B_4^1\} - \{B_4^{-1}\})], \\
 [B_4^{-3}] &= \frac{1}{2}(7\{B_4^2\} + 2\{B_4^{-4}\}), \\
 [B_4^{-4}] &= \frac{\sqrt{2}}{16} [(\{B_4^3\} + \{B_4^{-3}\}) + 7(\{B_4^1\} - \{B_4^{-1}\})].
 \end{aligned}$$

## References

- [1] S.V. Akimov, E.L. Mnushkina, E.F. Dudnik, *Sov. Phys.-Tech. Phys.* **27**, 500 (1982).
- [2] C. Manolikas, S. Amelinckx, *Phys. Status Solidi A* **60**, 167 (1980).
- [3] R.S. Roth, J.L. Waring, *Am. Mineral.* **48**, 1348 (1963).
- [4] J.D. Bierlein, A.W. Sleight, *Solid State Commun.* **16**, 69 (1975).
- [5] W.I.F. David, A.M. Glazer, A.W. Hewat, *Phase Transit.* **1**, 155 (1979).
- [6] A. Pinczuk, G. Burns, F.H. Dacol, *Solid State Commun.* **24**, 163 (1977).
- [7] A. Pinczuk, B. Welter, F.H. Dacol, *Solid State Commun.* **29**, 515 (1979).
- [8] M.S. Jang, H.L. Park, J.N. Kim, J.H. Ro, Y.H. Park, *Jpn. J. Appl. Phys.* **24**, 506 (1985).
- [9] S.H. Choh, E.Y. Moon, Y.H. Park, M.S. Jang, *Jpn. J. Appl. Phys.* **24**, 640 (1985).
- [10] E.Y. Moon, S.H. Choh, Y.H. Park, H.Y. Yeom, M.S. Jang, *J. Phys. C, Solid State Phys.* **20**, 1867 (1987).
- [11] A.R. Lim, S.H. Choh, M.S. Jang, *Ferroelectrics* **94**, 389 (1989).
- [12] A.R. Lim, S.H. Choh, M.S. Jang, *J. Phys., Condens. Matter* **4**, 1607 (1992).
- [13] N.P. Baran, V.I. Barchuk, V.G. Grachev, B.K. Krulikovskii, *Sov. Phys.-Crystallogr.* **30**, 410 (1985).
- [14] N.P. Baran, V.I. Barchuk, V.S. Vikhnin, *Sov. Phys.-Crystallogr.* **30**, 55 (1985).
- [15] N.P. Baran, V.I. Barchuk, V.G. Grachev, B.K. Krulikovskii, *Sov. Phys.-Solid State* **28**, 485 (1986).
- [16] T.H. Yeom, S.H. Choh, M.S. Jang, *J. Phys., Condens. Matter* **4**, 587 (1992).
- [17] J.R. Pilbrow, M.R. Lowrey, *Rep. Prog. Phys.* **43**, 18 (1980).
- [18] W.I.F. David, *J. Phys. C* **16**, 5127 (1983).
- [19] H. Tokumoto, H. Unoki, *Phys. Rev. B* **27**, 3748 (1983).
- [20] M. Cho, T. Yagi, T. Fujii, A. Sawada, Y. Ishibashi, *J. Phys. Soc. Japan* **51**, 2914 (1982).
- [21] L.P. Avakyants, A.M. Antonenko, E.F. Dudnik, D.F. Kiselev, I.E. Mnushkina, M.M. Firsova, *Sov. Phys.-Solid State* **24**, 1411 (1982).
- [22] A.W. Sleight, H.Y. Chen, A. Ferretti, D.E. Cox, *Mater. Res. Bull.* **14**, 1571 (1979).
- [23] I.G. Wood, A.M. Glazer, *J. Appl. Crystallogr.* **13**, 217 (1980).
- [24] S.A. Al'tshuler, B.M. Kozyrev, *Electron Paramagnetic Resonance in Compound of Transition Elements*, Wiley, New York 1968, Ch. 3.
- [25] C. Rudowicz, *J. Phys. C* **18**, 1415 (1985).
- [26] C. Rudowicz, *Magn. Reson. Rev.* **13**, 1 (1987).
- [27] C. Rudowicz, *J. Chem. Phys.* **86**, 5045 (1986).
- [28] S.K. Misra, C. Rudowicz, *Phys. Status Solidi B* **147**, 677 (1988).
- [29] C. Rudowicz, R. Bramley, *J. Chem. Phys.* **83**, 5192 (1985).
- [30] C. Rudowicz, *Mol. Phys.* **74**, 1159 (1991).
- [31] C. Rudowicz, *J. Magn. Reson.* **63**, 95 (1985).